

See discussions, stats, and author profiles for this publication at: <https://www.researchgate.net/publication/268787752>

# Toxicokinetic Toxicodynamic (TKTD) Modeling of Ag Toxicity in Freshwater Organisms: Whole-Body Sodium Loss Predicts Acute Mortality Across Aquatic Species

ARTICLE in ENVIRONMENTAL SCIENCE AND TECHNOLOGY · NOVEMBER 2014

Impact Factor: 5.33 · DOI: 10.1021/es504604w · Source: PubMed

CITATION

1

READS

61

## 5 AUTHORS, INCLUDING:



**Karin Veltman**

Radboud University Nijmegen

43 PUBLICATIONS 453 CITATIONS

SEE PROFILE



**Jan Hendriks**

Radboud University Nijmegen

208 PUBLICATIONS 3,587 CITATIONS

SEE PROFILE



**Mark A J Huijbregts**

Radboud University Nijmegen

239 PUBLICATIONS 5,797 CITATIONS

SEE PROFILE



**Olivier Jolliet**

University of Michigan

217 PUBLICATIONS 5,485 CITATIONS

SEE PROFILE

# Toxicokinetic Toxicodynamic (TKTD) Modeling of Ag Toxicity in Freshwater Organisms: Whole-Body Sodium Loss Predicts Acute Mortality Across Aquatic Species

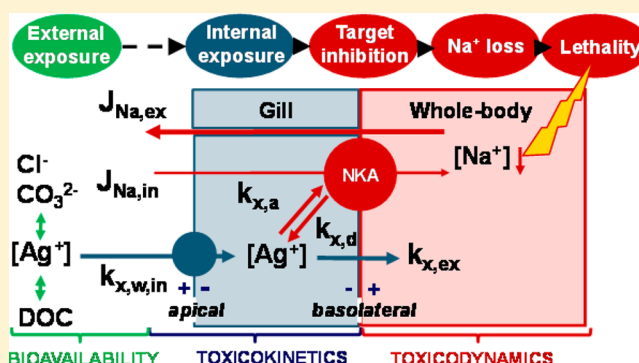
Karin Veltman,<sup>\*,†,‡</sup> A. Jan Hendriks,<sup>†</sup> Mark A. J. Huijbregts,<sup>†</sup> Cédric Wannaz,<sup>‡</sup> and Olivier Joliet<sup>‡</sup>

<sup>†</sup>Department of Environmental Science, Radboud University (RU), Nijmegen, The Netherlands

<sup>‡</sup>Department of Environmental Health Sciences (EHS), School of Public Health, University of Michigan, Ann Arbor, United States

## S Supporting Information

**ABSTRACT:** Toxicokinetic Toxicodynamic (TKTD) models are considered essential tools to further advance acute toxicity prediction of metals for a range of species and exposure conditions, but they are currently underutilized. We present a mechanistic TKTD model for acute toxicity prediction of silver (Ag) in freshwater organisms. In this new approach, we explicitly link relevant TKTD processes to species (physiological) characteristics, which facilitates model application to other untested freshwater organisms. The model quantifies the reduction in whole-body sodium concentration over time as a function of the target site inhibition over time, the target site density and the species-specific sodium turnover rate. Freshwater species are assumed to die instantly when they have lost a critical amount of their initial whole-body sodium concentration. Results show that mortality is significantly related to sodium loss ( $r^2 = 0.86$ ) for various aquatic organisms and exposure durations. The model accurately predicts lethal effect concentrations for different freshwater organisms, including *Daphnia magna*, rainbow trout and juvenile crayfish, and is able to capture the observed size-specific variation of nearly 2 orders of magnitude in empirical  $LC_{50}$ s.



## INTRODUCTION

A key challenge facing ecotoxicology is the need to assess the risk of thousands of substances, for a wide range of species, with high accuracy and ecological relevance. Toxicokinetic-Toxicodynamic (TKTD) models are advocated as essential tools for addressing this challenge.<sup>1,2</sup> However, their potential for extrapolation across species is currently underutilized. This mainly results from a lack of quantitative understanding of key biochemical and physiological processes that determine species sensitivity. It is thought that TKTD modeling can significantly advance if toxicodynamic parameters are quantitatively related to key species characteristics.<sup>1</sup> Here, we present such a mechanistic TKTD model for acute toxicity prediction of silver (Ag) in freshwater organisms.

In most freshwater organisms, Ag elicits its acute toxic action by inhibiting enzymes and proteins responsible for the uptake of sodium.<sup>3–6</sup> The toxic mechanism involves competition with  $Na^+$  at uptake sites (Na channels) on the apical surface of the gill membrane, inhibition of cellular carbonic anhydrase and noncompetitive inhibition of basolateral  $Na^+/K^+$ -ATPase (NKA). The inhibition of NKA initiates a cascade of detrimental molecular and physiological reactions, which can propagate to toxic effects at the organism level.<sup>3,7</sup> Specifically, the inhibition of NKA reduces the influx of sodium into the blood. Yet, the passive diffusive efflux of sodium via the

paracellular junctions continues, and the plasma sodium concentrations consequently fall below the optimum concentration. This plasma sodium loss causes a perturbed fluid-volume regulation, hemoconcentration, increased cardiac and ventilation rates, and ultimately organism death occurs due to cardiovascular collapse.<sup>6,8</sup>

A commonly used model in the environmental risk assessment of metals is the Biotic Ligand Model (BLM). The BLM predicts acute toxicity by accounting for metal speciation in the abiotic environment and competitive binding of protective cations at the site of toxic action (biotic ligand). Acute toxicity of a prescribed degree is assumed to occur when the accumulated metal on physiologically active sites (biotic ligands) in the gills of aquatic organisms equals a critical concentration ( $LA_{50}$ ).<sup>9</sup> The strength of the BLM is the explicit consideration of metal speciation in the ambient environment and competitive binding to the biotic ligand, which facilitates model application to different water chemistries.<sup>9,10</sup> The strong influence of physiological characteristics, such as size, on species sensitivity is not yet recognized by the BLM.

Received: September 19, 2014

Revised: November 20, 2014

Accepted: November 24, 2014

Published: November 24, 2014

Differences in sensitivity are generally dealt with by adjustments of BLM-parameters, such as the  $LA_{50}$ .<sup>10</sup>

It is well-known that considerable variation in sensitivity exists among species. Small organisms such as daphnids are often found to be 5–10 times more sensitive to metals than larger organisms, such as juvenile rainbow trout, in short-term assays.<sup>10</sup> Moreover, Bianchini et al.<sup>11</sup> and Grosell et al.<sup>12</sup> showed that  $LC_{50}$ s of Ag are significantly related to species size, which they attributed to the size-dependency of sodium loss rates.<sup>11,12</sup> Paquin et al.<sup>7</sup> developed a physiologically based ion model that predicts acute Ag toxicity in rainbow trout as a function of the sodium loss rate and the (equilibrium)  $LA_{50}$ . Rainbow trout were assumed to die instantly when they had lost 30% of their initial exchangeable sodium concentration. Grosell et al.<sup>12</sup> developed a physiologically based ion model to characterize species sensitivity to either Cu or Ag. The model predicts cumulative Na losses and time-to-death based on an assumed level of sodium uptake inhibition, but does not yet link the reduction in sodium influx to metal accumulation at the target site(s). At present, a comprehensive model that integrates key toxicokinetic and toxicodynamic processes is not yet available.

We aim to develop a mechanistic Toxicokinetic-Toxicodynamic model for acute toxicity prediction of Ag in freshwater organisms based on species (physiological) characteristics, target inhibition characteristics, and exposure conditions (concentration and duration). We develop a species-specific toxicodynamic model that quantifies and links the time-course of target enzyme inhibition with the time-course of whole-body sodium loss. A “sodium loss”-response curve is established that relates fraction/percentage sodium loss to fraction/percentage mortality for a range of species and exposure durations. The TD model is integrated with a previously developed mechanistic model for species-specific Ag uptake. The full TKTD model is predominantly parametrized based on literature-collected empirical data, but two remaining parameters are calibrated with time-course data for sublethal effects. The model is tested with an independent acute toxicity-data set covering several freshwater organisms of different size. To avoid complications due to water chemistry differences, we collected data for two water types specifically, that is, Hamilton tap water and soft water created from reverse osmosis of Hamilton tap water.

## MATERIALS AND METHODS

**Toxicokinetic-Toxicodynamic Model.** *Toxicokinetics.* Toxicokinetics links the external, bioavailable concentration ( $C_{x,ext}$ ,  $\mu\text{mol}_x \cdot \text{L}^{-1}$ ) to the total internal concentration in the target organ ( $C_{x,int,tot}$ ,  $\mu\text{mol}_x \cdot \text{L}^{-1}$ ). The dominant target site for Ag is NKA,<sup>5–7,11,13</sup> which is located at the basolateral site of the gill membrane. The gill Ag concentration can be quantified based on the Ag uptake rate across the apical membrane and the Ag efflux rate from the gill:

$$\frac{dC_{x,int,tot}}{dt} = k_{x,w,in} \cdot \frac{1}{F_{gill}} \cdot C_{x,ext} - k_{x,ex} \cdot (C_{x,int,tot} - NKA_{nf}) \quad (1)$$

$k_{x,w,in}$  = metal- and species-specific apical uptake rate constant ( $\text{L} \cdot \text{kg}_{\text{body wt.}}^{-1} \cdot \text{d}^{-1}$ )  $k_{x,ex}$  = species-specific efflux rate constant ( $\text{d}^{-1}$ )  $NKA_{nf}$  = concentration of nonfunctional target enzymes, which equals the concentration of Ag bound to NKA ( $\mu\text{mol}_x \cdot \text{L}^{-1}$ )  $F_{gill}$  = gill volume per kg whole-body weight ( $\text{L} \cdot \text{kg}_{\text{body wt.}}^{-1}$ )

The efflux rate is a function of the labile Ag concentration ( $C_{x,int,labile} = C_{x,int,tot} - NKA_{nf}$ ,  $\mu\text{mol}_x \cdot \text{L}^{-1}$ ), rather than the total gill Ag concentration, as Ag bound to NKA can, at that time, not be removed from the gill. Uptake rate constants commonly refer to the uptake per kg whole-body wet weight. We are, however, interested in quantifying the Ag concentration in the gill and uptake rates are therefore expressed as  $k_{x,w,in}/F_{gill}$  in  $\text{L}_{\text{water}} \cdot \text{L}_{\text{gill}}^{-1} \cdot \text{day}^{-1}$ .

Mechanistically, the uptake rate constant can be further delineated into the species-specific ventilation (or filtration) rate ( $k_{w,in}$ ,  $\text{L} \cdot \text{kg}^{-1} \cdot \text{d}^{-1}$ ) and the metal-specific absorption efficiency ( $p_{x,w,in}$ , (–)), as is commonly done in kinetic bioaccumulation models:<sup>14–16</sup>

$$k_{x,w,in} = p_{x,w,in} \cdot k_{w,in} \quad (2)$$

**Toxicodynamics.** The toxicodynamic model quantifies and links the time-dependent inhibition of the target sites (NKA) in the gill with the whole-body exchangeable sodium loss, which is in turn linked to organism mortality. The toxicodynamic model for target site inhibition is developed in analogy to the receptor kinetics model of Jager and Kooijman<sup>17</sup> for acetylcholinesterase inhibition by organophosphates. Ag is assumed to interact in a 1:1 stoichiometry with the target site,<sup>4</sup> that is, one mole of free Ag ( $\text{Ag}^+$ ) reacts with one mole of functional NKA enzymes ( $NKA_f$ ) to produce one mole of Ag–NKA complexes, which equals one mole of nonfunctional NKA enzymes ( $NKA_{nf}$ ) (eq 3).



$k_{x,a}$  = metal-specific association rate constant with the target enzyme ( $\text{L} \cdot \mu\text{mol}^{-1} \cdot \text{d}^{-1}$ )  $k_{x,d}$  = metal-specific dissociation rate constant from the target enzyme ( $\text{d}^{-1}$ )

An organism can initiate various defense mechanisms that lead to recovery of the target enzyme, including de novo production of enzymes. These mechanisms can be incorporated in a “recovery rate” ( $k_r$  in  $\text{d}^{-1}$ ), for example.<sup>2</sup> For short-term (acute) exposures it is assumed that recovery is negligible. The total concentration of NKA enzymes ( $NKA_{tot}$ ,  $\mu\text{mol} \cdot \text{L}^{-1}$ ) is thus constant and equals the initial concentration in unperturbed conditions ( $NKA_{(0)}$ ,  $\mu\text{mol} \cdot \text{L}^{-1}$ ):  $NKA_{tot} = NKA_{(0)} = NKA_{nf} + NKA_f$ . The concentration of nonfunctional target enzymes ( $NKA_{nf}$ ,  $\mu\text{mol}_{NKA_{nf}} \cdot \text{L}^{-1}$ ) over time can be described as a function of the labile Ag concentration in the gill, the concentration of free, noninhibited target enzymes ( $NKA_f = (NKA_{(0)} - NKA_{nf})$ ,  $\mu\text{mol}_{NKA_f} \cdot \text{L}^{-1}$ ), the association rate with the target enzyme ( $k_{x,a}$ ) and the dissociation rate from the target enzyme ( $k_{x,d}$ ):

$$\frac{dNKA_{nf}}{dt} = k_{x,a} \cdot (C_{x,int,tot} - NKA_{nf}) \cdot (NKA_{(0)} - NKA_{nf}) - k_{x,d} \cdot NKA_{nf} \quad (4)$$

The fraction of nonfunctional enzymes at a specific time-point can be quantified as

$$f_{nf}(t) = \frac{NKA_{nf}(t)}{NKA_{(0)}} \quad (5)$$

$f_{nf}(t)$  = fraction of nonfunctional target enzymes (–)

Inhibition of NKA enzymes results in a reduced active influx of sodium into the organism, which causes a reduction in

Table 1. Model Parameterization

	parameter	value	unit	reference
$p_{Ag,w,in}$	absorption efficiency for Ag	3.73%	[–]	16
$k_{w,in}$	ventilation rate (fish and large crustaceans)	$2.0 \times 10^2 \cdot w^{-0.25}$	$[L \cdot kg^{-1} \cdot d^{-1}]$	19
$k_{f,in}$	filtration rate (daphnids)	$6.0 \times 10^2 \cdot w^{-0.32}$	$[L \cdot kg^{-1} \cdot d^{-1}]$	20, 21
$k_{x,ex}$	efflux rate constant across the basolateral membrane ( $y_{ex} \cdot w^{-0.25}$ )	$1.03 \cdot w^{0.25}$	$[d^{-1}]$	calibrated
$F_{gill}$	volume of osmoregulatory organ (e.g., gill) per kg whole-body wet weight	$2.1 \times 10^{-2}$	$[L \cdot kg^{-1}]$	S2
$K_{x,D}$	dissociation constant for interaction of Ag with $Na^+/K^+$ -ATPase ( $k_{x,d}/k_{x,a}$ )	$1.6 \times 10^{-1}$	$[\mu mol \cdot L^{-1}]$	3
$k_{x,a}$	association rate constant for Ag association with $Na^+/K^+$ -ATPase ( $k_{x,d}/K_{x,D}$ )	$6.3 \times 10^2$	$[\mu mol \cdot L^{-1} \cdot d^{-1}]$	calibrated
$k_{x,d}$	dissociation rate constant for Ag dissociation from $Na^+/K^+$ -ATPase ( $K_{x,D} \cdot k_{x,a}$ )	$1.0 \times 10^2$	$[d^{-1}]$	calibrated
$J_{Na,max}$	whole-body maximum uptake rate of sodium from dechlorinated Hamilton tap water	$2.8 \times 10^3 \cdot w^{-0.31}$	$[\mu mol \cdot kg^{-1} \cdot d^{-1}]$	S3
$J_{Na,max}$	whole-body maximum uptake rate of sodium from soft water	$4.5 \times 10^3 \cdot w^{-0.37}$	$[\mu mol \cdot kg^{-1} \cdot d^{-1}]$	S3
$K_{M,HW}$	Michaelis Menten constant for Na uptake from dechlorinated Hamilton tap water (HW)	$1.5 \times 10^2$	$[\mu mol \cdot L^{-1}]$	S3
$K_{M,SW}$	Michaelis Menten constant for Na uptake from soft water (SW)	$5.4 \times 10^1$	$[\mu mol \cdot L^{-1}]$	S3
$k_{int}$	sodium internalization rate constant per molecule of $Na^+/K^+$ -ATPase (molecular turnover rate)	$5.1 \times 10^5$	$[d^{-1}]$	eq 7
$NKA_{(0),HW}$	concentration of $Na^+/K^+$ -ATPase enzymes in osmoregulatory organ under unperturbed conditions, for dechlorinated Hamilton tap water	$2.6 \times 10^{-1} \cdot w^{-0.31}$	$[\mu mol \cdot L^{-1}]$	S4
$NKA_{(0),SW}$	concentration of $Na^+/K^+$ -ATPase enzymes in osmoregulatory organ under unperturbed conditions, for soft water	$3.9 \times 10^{-1} \cdot w^{-0.37}$	$[\mu mol \cdot L^{-1}]$	S4
$k_{Na,ex}$	diffusive sodium efflux rate constant	species-specific	$[d^{-1}]$	eq 6
$C_{Na,int}$	whole-body exchangeable sodium concentration	species-, experiment-specific	$[\mu mol \cdot kg^{-1}]$	S7, S8 <sup>a</sup>
$C_{Na,ext}$	external sodium concentration (in water)	experiment-specific	$[\mu mol \cdot L^{-1}]$	S7, S8 <sup>a</sup>

<sup>a</sup>Experiment-specific or species-specific values are used when available, otherwise a mean (species-specific) value is used. Parameters in *italic* are calibrated.

exchangeable, whole-body sodium levels. In freshwater organisms, sodium uptake is an active transport process. Carrier-mediated transport is commonly described by Michaelis–Menten kinetics, that is, as a function of the maximum whole-body sodium uptake rate ( $J_{Na,max}$ ,  $\mu mol \cdot kg^{-1} \cdot d^{-1}$ ), the Michaelis constant for sodium uptake ( $K_M$ ,  $\mu mol \cdot L^{-1}$ ) and the external sodium concentration in water ( $C_{Na,ext}$ ,  $\mu mol \cdot L^{-1}$ ). Sodium efflux occurs by passive diffusion and is a function of the species-specific sodium efflux rate constant ( $k_{Na,ex}$ ,  $d^{-1}$ ) and the whole-body, exchangeable sodium concentration ( $C_{Na,int}$ ,  $\mu mol \cdot kg^{-1}$ ):

$$\frac{dC_{Na,int}}{dt} = (1 - f_{nf(t)}) \cdot \frac{J_{Na,max}}{K_M + C_{Na,ext}} \cdot C_{Na,ext} - k_{Na,ex} \cdot C_{Na,int} \quad (6)$$

The noncompetitive inhibition of sodium influx is characterized by the fraction of nonfunctional target enzymes. Under normal unperturbed conditions, when  $f_{nf} = 0$ , there is no inhibition of sodium uptake and when  $f_{nf} = 1$ , there is full inhibition of sodium uptake.

The maximum whole-body sodium influx rate can be further delineated into the initial concentration of NKA enzymes in the gill, the intrinsic sodium turnover rate constant ( $k_{int}$ ,  $d^{-1}$ ), and the gill volume per kg body weight:

$$J_{Na,max} = NKA_{(0)} \cdot k_{int} \cdot F_{gill} \quad (7)$$

This delineation is necessary as the initial concentration of NKA enzymes is not invariant across species (see below).

The reduction in exchangeable whole-body sodium concentrations is subsequently related to mortality. In analogy with Paquin et al.,<sup>7</sup> we assume that “instant” death occurs when an organism has lost a critical amount of sodium. The critical sodium loss threshold is thought to be around 30% for rainbow trout.<sup>7</sup> To determine whether this critical sodium loss threshold

is applicable to other freshwater species as well, we collected data on the fraction/percentage mortality and the associated fraction/percentage sodium loss for a range of aquatic species and exposure durations. We subsequently related %mortality to %sodium loss using the relationship from Janoschek.<sup>18</sup> The Janoschek-curve presents a sigmoidal, skewed curve with a minimum amount of fitting parameters:

$$\%mortality = A_{upp} - (A_{upp} - A_{low}) \cdot \exp(-(b \cdot \%Na_{loss})^c) \quad (8)$$

%mortality = mortality percentage in a specific test population (%)  
 $\%Na_{loss}$  = whole-body, exchangeable sodium loss (%)  
 $A_{upp}$  = upper asymptote (1) (–)  
 $A_{low}$  = lower asymptote (0) (–)  
 $b$  = fitted parameter  
 $c$  = fitted parameter

The mortality-curve can be used in the model to back-calculate time-specific lethal external effect concentrations for a specific fraction  $x$  of the test population ( $LC_x$ ).

**Parameterization, Calibration, and Evaluation.** *Parameterization.* All parameter values are provided in Table 1. Parameter values are obtained from a comprehensive literature review, except for the efflux rate constant ( $k_{x,ex}$ ) and the association rate constant ( $k_{x,a}$ ), which are calibrated. The Ag absorption efficiency is obtained from Veltman et al.<sup>16</sup> and is based on free ion concentrations. In previous studies, we showed that this absorption efficiency is metal-specific, but species-independent.<sup>15,16</sup> We therefore used a fixed value for all species. Ventilation (or filtration) rates are species-specific. Analogous to Veltman et al.<sup>15,16</sup> ventilation rates for fish species and large crustaceans are quantified as  $k_{w,in} = 200 \cdot w^{-\kappa}$ , where  $k_{w,in}$  is the water ventilation rate ( $L \cdot kg^{-1} \cdot d^{-1}$ ),  $w$  is the species wet weight (kg) and  $\kappa$  is the allometric scaling exponent (0.25).<sup>19</sup> For *Daphnia magna*, filtration rates are calculated from length-weight and length-filtration rate regressions (S1).<sup>20,21</sup> We collected data on gill volume per kg whole-body wet weight for different species from literature (S2). In



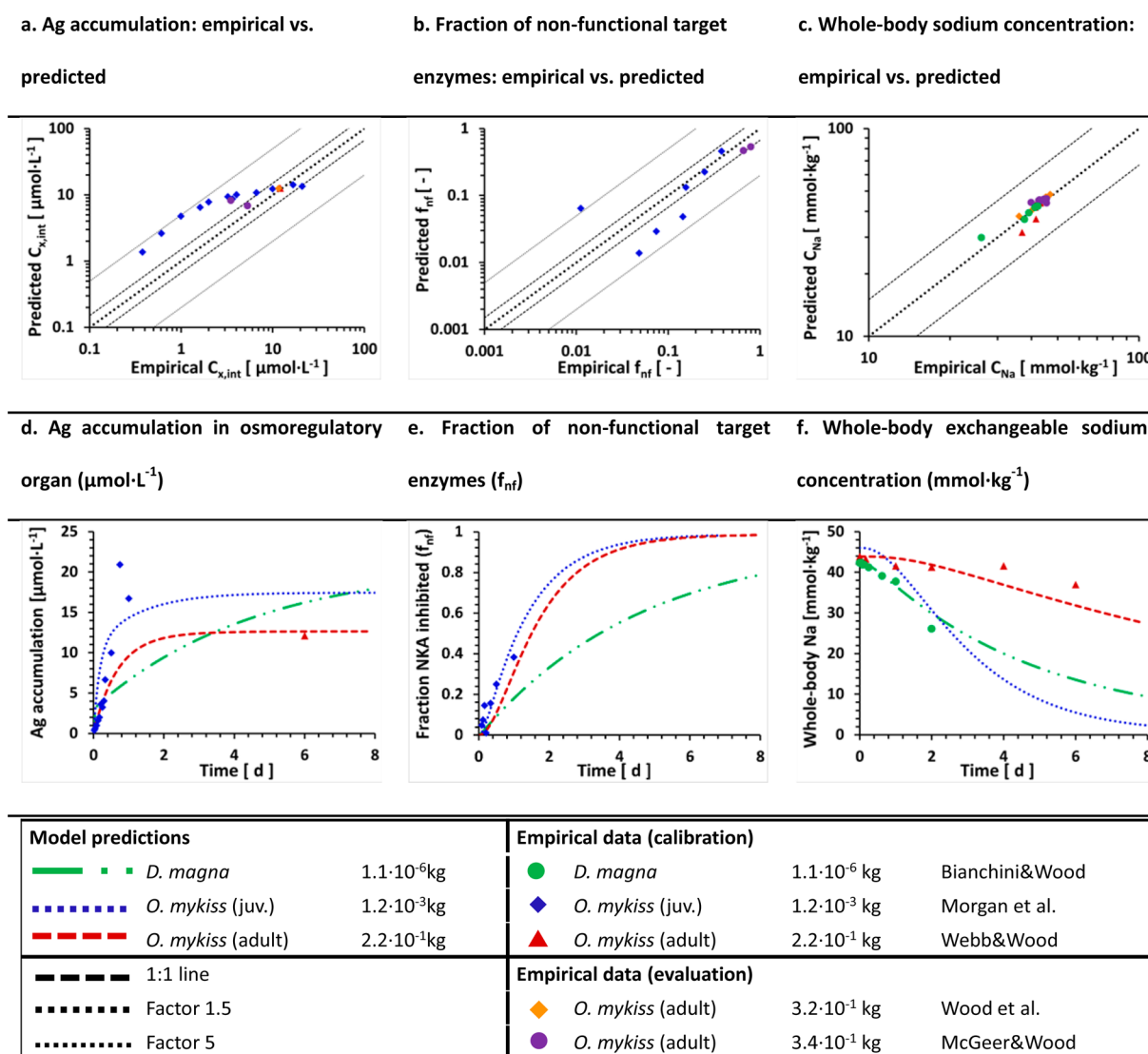


**Figure 1.** Model predictions and empirical data for three sublethal end points: gill Ag accumulation (total Ag) ( $C_{\text{x,int}}$ ), fraction of nonfunctional target enzymes ( $f_{\text{nf}}$ ) and whole-body sodium concentration ( $C_{\text{Na,int}}$ ).

analogy with pharmacokinetic modeling approaches,<sup>22</sup> we assume that organ volume fractions are invariant with body weight and a geometric mean value is used for all species. The mechanisms of metal efflux from the gill are presently not well understood<sup>23,24</sup> and this rate constant is therefore calibrated (see Calibration below).

Metal association rates ( $k_{\text{x,a}}$ ) and dissociation rates ( $k_{\text{x,d}}$ ) are not commonly measured. However, Morgan et al.<sup>3</sup> determined the  $\text{IC}_{50}$  for NKA inhibition by Ag in gill cells of rainbow trout.  $\text{IC}_{50}$ s represent the inhibitor concentration at which enzyme activity is reduced by 50% and are a measure of inhibitor potency.<sup>25</sup> For noncompetitive inhibitors,  $\text{IC}_{50}$  values equal the metal-specific equilibrium dissociation constant ( $K_{\text{x,D}} = k_{\text{x,d}}/k_{\text{x,a}}$ ) of the metal–NKA complex.<sup>25</sup> Experimental evidence suggests, however, that in vivo Ag interaction with basolateral NKA is not an “instantaneous” equilibrium reaction.<sup>26,27</sup> According to Morgan and Wood<sup>26</sup> “it can take anywhere from 5 to 24 h for the inhibitory effect of silver on  $\text{Na}^+/\text{K}^+$ –ATPase to develop fully.” We therefore calibrate the association rate constant on experimental data for target enzyme inhibition and sodium loss, knowing that  $k_{\text{x,a}}$  equals  $k_{\text{x,d}}/K_{\text{x,D}}$ .

Sodium influx rates ( $J_{\text{Na,in}}$ ) were collected for the two water types, that is, Hamilton tap water (HW) and soft water (SW), and for various aquatic organisms, including daphnids and several fish species. For each species, we additionally collected species weight and the initial exchangeable sodium concentration (S3). We developed water-type specific linear regressions of sodium influx rates and species weight, as sodium influx rates are known to be water chemistry dependent (S3).<sup>7,28</sup> We also collected water-chemistry specific  $K_{\text{M}}$ -values. For Hamilton tap water,  $K_{\text{M}}$  values were obtained for *Daphnia magna* and rainbow trout. A geometric mean value was calculated and used for all species (S3). For soft water, we obtained a  $K_{\text{M}}$ -value for rainbow trout from Bury et al.,<sup>23</sup> which was determined in water of the same water chemistry. The water type-specific  $K_{\text{M}}$ -values are used to calculate water type-specific maximum influx rates ( $J_{\text{Na,max}}$ ) based on the regressions for  $J_{\text{Na,in}}$  and eq 6. Subsequently, water type-specific and species-specific sodium efflux rate constants ( $k_{\text{Na,ex}}$ ) were calculated (eq 6).

McCormick and Bern<sup>29</sup> measured the NKA density in the gill of presmolt juvenile coho salmon using [ $^3\text{H}$ ]ouabain binding. A NKA density of 4.2 pmol NKA/mg gill dry tissue was found,

which corresponds to a NKA density of  $8.4 \times 10^{-1} \mu\text{mol} \cdot \text{L}_{\text{gill}}^{-1}$  for a fish of  $2.4 \times 10^{-2} \text{ kg}$  (S4). Based on the allometric relationship for  $J_{\text{Na,max}}$ , a sodium internalization rate constant ( $k_{\text{int}}$ ) of  $5.5 \times 10^5 \text{ d}^{-1}$  is found. This internalization rate constant represents the sodium turnover per molecule of NKA per day, which is assumed to be constant for all freshwater organisms. As the gill volume per kg body weight is also constant across species, the NKA concentration in the gill is consequently species-specific (eq 6,7).

We collected the fraction/percentage mortality and the associated fraction/percentage sodium loss data from literature for a range of aquatic species and exposure durations (S5). This type of data is sparsely available for Ag, however, sufficient data exist for copper. As copper is known to have a similar toxic mechanism of action as Ag,<sup>8,30</sup> these data were used here. The Janoschek-curve (eq 8) was fitted to empirical data using linear-least-squares fitting with the Excel Solver.

**Calibration.** The efflux rate constant ( $k_{\text{x,ex}}$ ) and the association rate constant ( $k_{\text{x,a}}$ ) were fitted on empirical time-course data for gill Ag accumulation, NKA inhibition and whole-body exchangeable sodium loss using linear-least-squares fitting (Figure 1a–c). The model was implemented in Sysquake 5 (www.calerga.com) and solved numerically. We collected time-course data for NKA inhibition and whole-body sodium loss for the two water types used. If gill Ag accumulation was measured in the same study, these data were collected as well. If necessary, free ion concentrations were calculated using VisualMINTEQ 3.0. Time-course data for NKA inhibition and Na loss were found in five studies, that is, Bianchini and Wood,<sup>5</sup> Wood et al.,<sup>8</sup> Morgan et al.,<sup>27</sup> Webb and Wood,<sup>31</sup> McGeer and Wood<sup>13</sup> (S7). From the McGeer and Wood-study,<sup>13</sup> we collected data that were obtained at the two lowest chloride concentrations only (i.e., 20 and 120  $\mu\text{mol Cl}^{-1} \cdot \text{L}^{-1}$ ) to ensure similarity in chloride water chemistry with the other soft water-studies (50  $\mu\text{mol Cl}^{-1} \cdot \text{L}^{-1}$ ). Most studies focused on adult rainbow trout. To avoid overrepresentation of adult rainbow trout in the data set, we selected the study with the longest time-course data for adult rainbow trout, that is, Webb and Wood.<sup>31</sup> The other studies, that is, Wood et al.,<sup>8</sup> McGeer and Wood<sup>13</sup> are used in the model evaluation. We thus have three model scenarios (i.e., gill Ag accumulation, NKA inhibition and sodium loss) with time-course data for two species of three distinct weights, that is, *D. magna*, juvenile rainbow trout and adult rainbow trout. The model was fitted on all three scenarios and all species simultaneously by normalizing all data and by accounting for the number of data per scenario (S6).

**Evaluation.** We compared model predictions with independent (time-course) data for enzyme inhibition and sodium loss in adult rainbow trout. Model performance is further evaluated with an independent acute toxicity data set. Acute toxicity data were collected from Bianchini et al.<sup>11</sup> who measured acute Ag toxicity for several freshwater species of different size in Hamilton tap water. They additionally measured sodium influx rates and provide measured species weights.<sup>11</sup> The Bianchini-data set thus forms a consistent data set to test our model.

## RESULTS

**Calibration.** Model calibration on sublethal effect data results in an efflux rate constant of  $1.03 \cdot w^{-0.25} \text{ d}^{-1}$  and an association rate of  $6.3 \times 10^{-2} \mu\text{mol} \cdot \text{L}^{-1} \cdot \text{d}^{-1}$ . The model accurately predicts whole-body exchangeable sodium loss over time for both *D. magna* and adult rainbow trout (Figure 1c,f).

All model predictions are within a factor of 1.2 from empirical data (Figure 1c). Gill Ag accumulation and target enzyme inhibition is less well predicted. The model overpredicts gill Ag accumulation in juvenile rainbow trout in the first 5 h of exposure (maximum factor 4.8 deviation), but shows better predictions for longer exposure durations, that is, from 8 until 24 h of exposure (Figure 1a,d). Gill Ag accumulation is well predicted (within a factor of 2.3) in adult rainbow trout after 50 h exposure (McGeer & Wood<sup>13</sup>), and after 6 days of exposure (Webb & Wood,<sup>31</sup> Wood et al.<sup>8</sup>). The model predicts the time-course of NKA inhibition reasonably well for juvenile rainbow trout (Figure 1b,e). All predictions are within a factor 3.5 from empirical data, except for two predictions at 1 and 5 h of exposure. At 1 h exposure, empirical data show a 7% increase in NKA activity compared to the original value. Such an increase in activity cannot be captured by the present model version and NKA inhibition is overestimated with a factor 18. At 5 h of exposure, a sudden drop in NKA inhibition is observed from ~15% inhibition at 4 h to ~1% inhibition at 5 h. Inhibition returns to 16% at 8 h of exposure. This unexpected pattern cannot be predicted by the model and NKA inhibition at 5 h exposure is overestimated with a factor 5.8. Target enzyme inhibition is well predicted for the adult rainbow trout (McGeer & Wood<sup>13</sup>). Predictions are within a factor 1.5 of empirical data.

**Sublethal Effects.** Figure 1 (d,e,f) shows the predicted time-course of sublethal effects for *D. magna* ( $1.1 \times 10^{-6} \text{ kg}$ ), juvenile rainbow trout ( $1.2 \times 10^{-3} \text{ kg}$ ) and adult rainbow trout ( $2.2 \times 10^{-1} \text{ kg}$ ). In both juvenile and adult rainbow trout, Ag accumulation reaches a steady-state value in approximately 3 days (Figure 1a). For *D. magna*, a rapid, nearly linear increase in Ag accumulation is predicted in the first 2 h of exposure. In contrast to the rainbow trout, gill Ag accumulation in *D. magna* does not level off to a steady-state value as the target enzymes of *D. magna* are not completely inhibited within 8 days of exposure. Such a long exposure duration is, however, practically unrealistic as 100% mortality would occur within 3 days of exposure for *D. magna* at this specific exposure concentration.

The time-course of NKA inhibition does not mimic the time-course of gill Ag accumulation (Figure 1e). For adult and juvenile rainbow trout, full inhibition occurs within 5 days of exposure. For *D. magna*, full inhibition is not reached within this period due to the lower external exposure concentration and the higher predicted NKA concentration in the gill. Species-specific differences in sodium loss rates result in differently shaped curves for whole-body exchangeable sodium loss for juvenile and adult rainbow trout (Figure 1f.) Despite a similar time-course of NKA inhibition, juvenile rainbow trout loses whole-body sodium at a faster rate than adult rainbow trout, because of the higher weight-specific sodium efflux rate in juveniles compared to adults.

**Lethal-Effects.** Whole-body exchangeable sodium loss is significantly related to mortality of freshwater organisms ( $r^2 = 0.86$ , RMSE = 0.14) (Figure 2). A sodium loss of 40% of the initial value is predicted to result in 50% mortality. The model accurately predicts time-specific  $\text{LC}_{50}$ s for a range of freshwater organisms of different size (Figure 3). Model predictions are within a factor of 2.1 from empirical data. For adult crayfish (weight  $1.9 \times 10^{-2} \text{ kg}$ ) the model cannot predict a 96 h  $\text{LC}_{50}$  as sodium loss in this large organism is too slow to result in a 40% loss within 96 h. Using the measured  $\text{LC}_{50}$  value, the model predicts that 50% mortality for adult crayfish occurs in 108 h of exposure. If exposure duration and concentration are

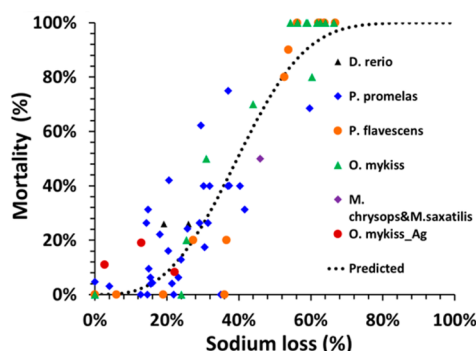


**Figure 2.** Mortality (%) as a function of sodium loss (%). %mort =  $1 - \exp(-11.7 \cdot \%Na_{loss}^{3.0})$ ,  $r^2 = 0.86$ , RMSE = 0.14.

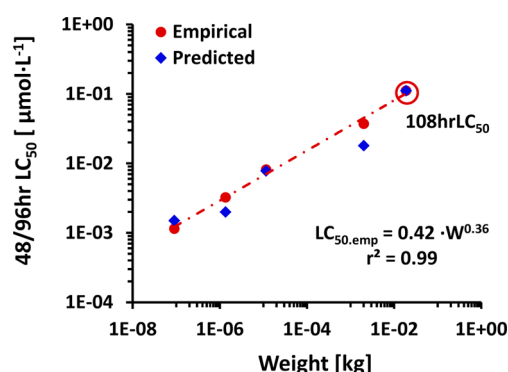


**Figure 3.** Predicted external toxicity values ( $LC_{50}$ ) and measured external toxicity values vs species weight.

completely interchangeable, this prediction is within a factor of 1.1 from empirical data. Figure 3 additionally shows that the model captures the size-specific scaling of  $LC_{50}$ s, that is,  $LC_{50}$ s are predicted to increase as a function of species size.

## DISCUSSION

**Predictions.** We predict gill Ag accumulation based on first-order kinetics. Gill metal accumulation is, however, known to be mediated by (multiple) carriers,<sup>4,24</sup> suggesting that Michaelis–Menten kinetics would have been more appropriate. However, as quantitative data on carrier-mediated transport of metal ions across the apical membrane is presently not available for a range of freshwater species, we chose to use a relatively simple model approach. Deviations from first-order kinetics can potentially explain the overprediction of gill Ag accumulation in juvenile rainbow trout in the first 5 h of exposure. Model predictions improve at longer exposure durations (>8 h–144 h), which is probably the most relevant exposure phase for acute toxicity predictions. It should be noted that our calibrated efflux rate constant integrates all removal processes from the gill, including metal extrusion across the basolateral membrane into the systemic circulation and metal extrusion across the apical membrane back into the external medium. Our modeling approach implicitly considers Ag binding to other ligands than NKA in the gill, such as metallothionein and –SH groups on enzymes and proteins in general. We used a Ag–NKA dissociation constant that is obtained from a gill homogenate assay for rainbow trout rather than a dissociation constant obtained from a purified enzyme assay. This implies that in our model approach the gill composition of all included freshwater species is comparable to the gill composition of rainbow trout

and that the “other ligands”: NKA ratio is comparable across species.

In contrast to the BLM, we assume that metal-target inhibition is not in thermodynamic equilibrium. An association rate constant of  $6.3 \times 10^{-2} \mu\text{mol} \cdot \text{L}^{-1} \cdot \text{d}^{-1}$  was obtained, which gives a dissociation rate constant of  $0.01 \text{ d}^{-1}$ . In the absence of repair mechanisms, this suggests a relatively slow recovery of NKA activity after full inhibition. The predicted time-course of NKA inhibition is generally consistent with empirical observations for juvenile rainbow trout except for the unexpected drop in NKA inhibition at 5 h of exposure.<sup>27</sup> This might be an experimental error or a one-time repair event. Metz et al.<sup>32</sup> suggested that “an intact cell may contain a latent pool of membrane vesicles carrying the enzyme that could be released”. This would result in a one-time increase in NKA activity, but not in a structural repair, which is consistent with empirical data from Morgan et al.<sup>27</sup> This shows that time-course data on NKA inhibition, and to lesser extent on Ag gill accumulation, are indispensable for a better prediction of NKA inhibition and to further advance toxicodynamic modeling of Ag in aquatic organisms.

The model accurately predicts time-specific  $LC_{50}$ s for various freshwater organisms. The 96h $LC_{50}$  for rainbow trout is slightly underestimated with a factor of 2.1. This may be attributed to the rainbow trout toxicity tests being performed under static-renewal conditions rather than under flow-through conditions, as used in all other experiments.  $LC_{50}$ s determined in static renewal tests are known to be higher than  $LC_{50}$ s in flow-through experiments due to a decrease in external Ag concentrations under static conditions.<sup>33</sup> The model is able to reflect the observed scaling of  $LC_{50}$ s with species weight. The allometric scaling of  $LC_{50}$ s of Ag, and also Cu, is commonly attributed to the size-dependency of sodium loss rates.<sup>11,12</sup> Here, we show, for the first time, that there is not a single rate-limiting step that determines the allometric scaling of external effect concentrations. The size-dependency of  $LC_{50}$ s is a function of both toxicokinetic and toxicodynamic processes. The species-specific sodium loss rate is an important factor, but the kinetics of NKA inhibition and the species-specific NKA concentrations also play an important role.

**Uncertainties.** A key uncertainty in our modeling approach relates to the imperfect (quantitative) knowledge on osmoregulatory processes for a range of freshwater organisms. Specifically the volume fraction of the gill ( $F_{\text{gill}}$ ), the initial concentration of NKA enzymes ( $NKA_{(0)}$ ), and the molecular turnover rate of the sodium pump ( $k_{\text{int}}$ ) are uncertain. We assumed that the gill volume fraction is invariant with body size and species independent. Although this is a common assumption in pharmacokinetic modeling,<sup>22,34</sup> it is not necessarily correct. Intraspecies (ontogenetic) scaling of gill volume fractions has been shown in some studies. For example, Garnier-Laplace et al.<sup>35</sup> showed that gill mass fraction (wet mass incl. bones) scales to whole-body wet weight to the power  $-0.12$  for rainbow trout. In contrast, the data of Huang et al.<sup>36</sup> for crucian carp show a positive scaling of gill fraction with whole-body mass (scaling exponent 0.14). Our own collected data show variability of gill volume fractions among species, but no significant correlation with weight ( $p > 0.19$ ), and we therefore choose to use a geometric mean value ( $S_2$ ).

The assumption of an invariant gill volume fraction implies that the NKA concentration in the gill scales to species weight to the power  $-0.31$  (for Hamilton tap water). Small organisms, such as *D. magna*, thus have a higher NKA concentration than



larger organisms, such as adult rainbow trout. At present, the NKA concentration has been measured in the gill of a few fish species only, that is, coho salmon, and three freshwater-acclimated marine species (*Fundulus heteroclitus*, *Mugil cephalus*, *Platichthys flesus*).<sup>29,37–39</sup> These limited data show a variable NKA concentration per kg gill wet weight, but no allometric scaling (S4). The scaling of NKA concentration is a key model parameter in our approach as it determines the lower-than-expected whole-body sodium loss for *D. magna*. The predicted time-pattern of sodium loss in *D. magna* is highly comparable to the observed (empirical) time-pattern of sodium loss (Figure 1f), which suggests a correct prediction of the NKA concentration in this small crustacean. These two assumptions, that is, an invariant “gill” volume fraction and an allometric scaling of NKA concentration, imply that the molecular turnover rate of the sodium pump ( $k_{\text{int}}$ ) is constant across species. This is consistent with Else et al.,<sup>40</sup> who showed that molecular turnover rates are relatively constant across a wide range of ectothermic species, including reptiles, amphibians and fish. Differences in molecular activity were observed, but these were mainly attributable to tissue-type.<sup>40</sup> The molecular turnover rate obtained, that is,  $5.5 \times 10^5 \text{ d}^{-1}$ , is comparable to the maximum molecular turnover rate determined for other ectotherms at 37 °C (range  $2.2 \times 10^6 - 3.6 \times 10^6 \text{ d}^{-1}$ , various tissues).<sup>40</sup>

In our model approach, we assume that the reduction in sodium influx is solely attributable to NKA inhibition. It is generally accepted that NKA is the key target site of silver.<sup>5–7,11,13</sup> Some studies have, however, suggested that inhibition of other enzymes involved in Na uptake, particularly carbonic anhydrase (CA), can contribute to the reduction in sodium influx.<sup>3,12,27</sup> Morgan et al.<sup>3</sup> and Morgan et al.<sup>27</sup> showed that Ag inhibits both carbonic anhydrase (CA) and NKA in rainbow trout, although CA appears to be inhibited to a lesser degree than NKA, that is, 28% vs 85%, respectively.<sup>3</sup> Morgan et al.<sup>27</sup> showed that sodium influx in rainbow trout exposed to Ag in soft water is immediately reduced (within 1 h), whereas  $\text{Na}^+/\text{K}^+$ -ATPase activity was not significantly inhibited until 24 h of exposure. They attribute the early decline of Na uptake to the inhibition of CA, and mention that the “later decline is probably related to  $\text{Na}^+/\text{K}^+$ -ATPase blockade”.<sup>27</sup> Unfortunately, the relative contributions of CA inhibition and NKA inhibition to the total reduction in Na uptake, and the relevancy of this mechanism of action in longer exposure durations (i.e., 96 h), other water chemistries (hard water), and other species, are not yet known. Including CA inhibition in our model might improve model predictions, particularly in terms of short-term inhibition. Further experimental evidence of CA inhibition and detailed time-course analyses of CA inhibition and sodium loss in a range of species and water chemistries, are, however, required to incorporate this pathway in a mechanistic model.

A premise of the model is that acute toxicity of freshwater organisms can be predicted from a generic sodium loss-mortality curve. The sodium loss-mortality curve was established based on empirical data for five aquatic species, two metals (i.e., Cu and Ag) and different exposure durations, suggesting that the assumption of a species-, metal-, and exposure time-independent “critical sodium loss threshold” is correct. A plot of the residuals against species weight shows no relation with weight (S5), suggesting no allometric scaling of the sodium loss threshold. The variability is, however, relatively large. This is partly due to experimental variability: there is no standardized way to measure sodium loss and some studies

determine %sodium loss in survivors at a specific time point whereas determine %sodium loss in organisms at the time-of-death. Further empirical research should focus on determining mortality fractions and associated sodium loss fractions for a wider range of species, particularly including crustaceans, and standard conditions.

Finally, in analogy with the BLM, we assume that repair, that is, de novo synthesis of NKA and metal detoxification by, for example, metallothionein (MT) induction, is not occurring under acute exposure conditions. It has been shown that repair mechanisms can be induced at chronic exposure, resulting in a decrease in toxic response over time.<sup>41–43</sup> The relevance of repair mechanisms in acute exposures is not well-known. The empirical data on NKA inhibition and sodium loss show no systematic decrease in toxic response over time (Figure 1). Accordingly, Monteiro et al.<sup>44</sup> showed that inhibition of gill NKA by Cu in *Oreochromis niloticus* was an early event (within 3 days) and steadily sustained, thus confirming the absence of compensatory processes going on in the gill. It is likely that the system is overwhelmed in acute exposures, which limits the possibility for inducing compensating repair mechanisms.

**Applicability and Implications.** We propose a mechanistic TKTD model that predicts acute toxicity of Ag in freshwater organisms as a function of species physiological characteristics, target site characteristics, and exposure conditions (concentration and duration). Most current TKTD models are based on whole-body concentrations. Here, we explicitly link the time-dependent inhibition of the molecular target (NKA), with the toxic response at the organism-level. Another novel aspect of our approach is that we explicitly link TK and TD processes to relevant species physiological characteristics (e.g., size) which allows for extrapolation to other freshwater organisms. The model is thought to be applicable to “all” freshwater organisms, provided that “osmoregulation” and “respiration” are linked to the same organ. The model is not directly applicable to species where osmoregulation and metabolism are decoupled, such as early fish larvae and (some) aquatic insects.<sup>45,46</sup> Regressions of acute Ag toxicity with species size, for example, refs 11 and 12 could also be used to predict acute Ag toxicity for other freshwater organisms. Our model approach does, however, have several merits compared to a regression: First, our model is applicable to different conditions, whereas regressions are generally applicable only to the (narrow) conditions under which they were derived. Our model can, for example, be applied to different exposure durations, as time is explicitly considered. Also, while our model is presently parametrized for Ag specifically, the framework is generic and a similar approach can be followed for other metals that elicit their toxic action by inhibition of NKA, such as copper, and potentially Ag-nanoparticles.<sup>47</sup> Second, a mechanistic model facilitates the incorporation of new, mechanistic knowledge, for example, the inhibition of carbonic anhydrase and its effect on Na influx, into the model. Finally, the developed model provides a mechanistic explanation of the observed toxic response pattern over time and can provide new insights in the toxic mechanism of action.

Our study has implications for the BLM and for TKTD modeling in general. We show that a one compartment equilibrium framework, such as employed by the BLM, is not sufficient to quantify acute metal toxicity for different species and exposure durations. Consideration of both toxicokinetics, that is, uptake and elimination kinetics, and toxicodynamics, that is, target enzyme inhibition dynamics and physiological



effects, are essential for extrapolation across species and exposure durations. TKTD models are considered powerful tools for a more scientifically based extrapolation of toxicity metrics across species, for example, refs 1, 2. Our results indicate that an accurate estimation of the target site concentration is essential to determine differences in species sensitivity. Time-course data of target site inhibition and consequential physiological effects are essential for model parametrization.

## ■ ASSOCIATED CONTENT

### ■ Supporting Information

The SI tabulates all collected data and additional information and figures on the sodium mass-balance model. This material is available free of charge via the Internet at <http://pubs.acs.org>.

## ■ AUTHOR INFORMATION

### Corresponding Author

\*Phone: +1 (734) 353-6735; fax: +1 (734) 763-8095; e-mail: [veltmank@umich.edu](mailto:veltmank@umich.edu).

### Notes

The authors declare no competing financial interest.

## ■ ACKNOWLEDGMENTS

KV is partly funded by a Marie-Curie Intra-European fellowship (IEF) (MEMOCTR, project no. 273104).

## ■ REFERENCES

- (1) Ashauer, R.; Escher, B. I. Advantages of toxicokinetic and toxicodynamic modelling in aquatic ecotoxicology and risk assessment. *J. Environ. Monitor.* **2010**, *12*, 2056–2061.
- (2) Jager, T.; Albert, C.; Preuss, T. G.; Ashauer, R. General unified threshold model of survival—A toxicokinetic-toxicodynamic framework for ecotoxicology. *Environ. Sci. Technol.* **2011**, *45*, 2529–2540.
- (3) Morgan, I. J.; Henry, R. P.; Wood, C. M. The mechanism of acute silver nitrate toxicity in freshwater rainbow trout (*Oncorhynchus mykiss*) is inhibition of gill  $\text{Na}^+$  and  $\text{Cl}^-$  transport. *Aquat. Toxicol.* **1997**, *39*, 145–163.
- (4) Wood, C. M.; Playle, R. C.; Hogstrand, C. Physiology and modeling of mechanisms of silver uptake and toxicity in fish. *Environ. Toxicol. Chem.* **1999**, *18*, 71–83.
- (5) Bianchini, A.; Wood, C. M. Mechanism of acute silver toxicity in *Daphnia magna*. *Environ. Toxicol. Chem.* **2003**, *22*, 1361–1367.
- (6) Grosell, M.; Brauner, C. J.; Kelly, S. P.; McGeer, J. C.; Bianchini, A.; Wood, C. M. Physiological responses to acute silver exposure in the freshwater crayfish (*Cambarus diogenes diogenes*)—A model invertebrate? *Environ. Toxicol. Chem.* **2002**, *21*, 369–374.
- (7) Paquin, P. R.; Zoltay, V.; Winfield, R. P.; Wu, K. B.; Mathew, R.; Santore, R. C.; DiToro, D. M. Extension of the Biotic Ligand Model for acute toxicity to a physiologically-based model of the survival time of rainbow trout (*Oncorhynchus mykiss*) exposed to silver. *Comp. Biochem. Physiol. Part C* **2002**, *133*, 305–343.
- (8) Wood, C. M.; Hogstrand, C.; Galvez, F.; Munger, R. S. The physiology of waterborne silver toxicity in freshwater rainbow trout (*Oncorhynchus mykiss*) 1. The effects of silver nitrate. *Aquat. Toxicol.* **1996**, *35*, 93–109.
- (9) DiToro, D. M.; Allen, H. E.; Bergman, H. L.; Meyer, J. S.; Paquin, P. R.; Santore, R. C. Biotic ligand model of acute toxicity of metals. 1. Technical basis. *Environ. Toxicol. Chem.* **2001**, *20*, 2383–2396.
- (10) Niyogi, S.; Wood, C. M. Biotic Ligand Model. A flexible tool for developing site-specific water quality guidelines for metals. *Environ. Sci. Technol.* **2004**, *38*, 6177–6192.
- (11) Bianchini, A.; Grosell, M.; Gregory, S. M.; Wood, C. M. Acute silver toxicity in aquatic animals is a function of sodium uptake rate. *Environ. Sci. Technol.* **2002**, *36*, 1763–1766.
- (12) Grosell, M.; Nielsen, C.; Bianchini, A. Sodium turnover rate determines sensitivity to acute copper and silver exposure in freshwater animals. *Comp. Biochem. Physiol. Part C: Toxicol. Pharmacol.* **2002**, *133*, 287–303.
- (13) McGeer, J. C.; Wood, C. M. Protective effects of water  $\text{Cl}^-$  on physiological responses to waterborne silver in rainbow trout. *Can. J. Fish. Aquat. Sci.* **1998**, *55*, 2447–2453.
- (14) Wang, W.-X. Comparison of metal uptake rate and absorption efficiency in marine bivalves. *Environ. Toxicol. Chem.* **2001**, *20*, 1367–1373.
- (15) Veltman, K.; Huijbregts, M. A. J.; van Kolck, M.; Wang, W.-X. Metal bioaccumulation in aquatic species: Quantification of uptake and elimination kinetics using physicochemical properties of metals. *Environ. Sci. Technol.* **2008**, *42*, 852–858.
- (16) Veltman, K.; Huijbregts, M. A. J.; Hendriks, A. J. Integration of biotic ligand models (BLM) and bioaccumulation kinetics into a mechanistic framework for metal uptake in aquatic organisms. *Environ. Sci. Technol.* **2010**, *44*, 5022–5028.
- (17) Jager, T. J.; Kooijman SALM. Modeling receptor kinetics in the analysis of survival data for organophosphorous pesticides. *Environ. Sci. Technol.* **2005**, *39*, 8307–8314.
- (18) Janoschek, A. Das reaktionskinetische Grundgesetz und seine Beziehungen zum Wachstums- und Ertragsgesetz. *Stat. Vjschr.* **1957**, *10*, 25–37.
- (19) Hendriks, A. J.; Heikens, A. The power of size. 2. Rate constants and equilibrium ratios for accumulation of inorganic substances related to species weight. *Environ. Toxicol. Chem.* **2001**, *20*, 1421–1437.
- (20) Burns, C. W. Relation between filtering rate, temperature, and body size in four species of *Daphnia*. *Limnol. Oceanogr.* **1969**, *14*, 693–700.
- (21) Knoechel, R.; Holtby, L. B. Construction and validation of a body-length-based model for the prediction of cladoceran community filtering rates. *Limnol. Oceanogr.* **1986**, *14*, 693–700.
- (22) Hayton, W. L.; Schultz, I. R. *Scaling Bioconcentration and Pharmacokinetic Parameters for Body Size and Environmental Variables in Fish. Aquatic Toxicology and Risk Assessment*, Fourteenth Vol. ASTM STP 1124; Mayes, M. A., Eds.; American Society for Testing and Materials: Philadelphia, 1991; pp 149–165.
- (23) Bury, N. R.; Grosell, M.; Grover, A. K.; Wood, C. M. ATP-dependent silver transport across the basolateral membrane of rainbow trout gill. *Toxicol. Appl. Pharmacol.* **1999**, *159*, 1–8.
- (24) Handy, R. D.; Eddy, F. B.; Baines, H. Sodium-dependent copper uptake across epithelia: A review of rationale with experimental evidence from gill and intestine. *Biochim. Biophys. Acta* **2002**, *1566*, 104–115.
- (25) Cheng, Y.-C.; Prusoff, W. H. Relationship between the inhibition constant ( $K_i$ ) and the concentrations of inhibitor which causes 50% inhibition ( $I_{50}$ ) of an enzymatic reaction. *Biochem. Pharmacol.* **1973**, *22*, 3099–3108.
- (26) Morgan, T. P.; Wood, C. M. A relationship between gill silver accumulation and acute silver toxicity in the freshwater rainbow trout: Support for the acute silver biotic ligand model. *Environ. Toxicol. Chem.* **2004**, *23*, 1261–1267.
- (27) Morgan, T. P.; Grosell, M.; Gilmour, K. M.; Playle, R. C.; Wood, C. M. Time course analysis of the mechanism by which silver inhibits active  $\text{Na}^+$  and  $\text{Cl}^-$  uptake in gills of rainbow trout. *Am. J. Physiol. Regul. Integr. Comp. Physiol.* **2004**, *287*, R234–R242.
- (28) Boisen, A. M. Z.; Amstrup, J.; Novak, I.; Grosell, M. Sodium and chloride transport in soft water and hard water acclimated zebrafish (*Danio rerio*). *Biochim. Biophys. Acta* **2003**, *1619*, 207–218.
- (29) McCormick, S. D.; Bern, H. A. *In vitro* stimulation of  $\text{Na}^+/\text{K}^+$ -ATPase activity and ouabain binding by cortisol in coho salmon gill. *Am. J. Physiol. Regul. Integr. Comp. Physiol.* **1989**, *256*, 707–715.
- (30) Laurén, D. J.; McDonald, D. G. Effects of copper on branchial ionoregulation in the rainbow trout, *Salmo gairdneri* Richardson. *J. Comp. Physiol. B* **1985**, *155*, 635–644.
- (31) Webb, N. A.; Wood, C. M. Physiological analysis of the stress response associated with acute silver nitrate exposure in freshwater

rainbow trout (*Oncorhynchus mykiss*). *Environ. Toxicol. Chem.* **1998**, *17*, 579–588.

(32) Metz, J. R.; van den Burg, E. H.; Wendelaar Bonga, S. E.; Flik, G. Regulation of branchial  $\text{Na}^+/\text{K}^+$ -ATPase in common carp *Cyprinus carpio* L. acclimated to different temperatures. *J. Exp. Biol.* **2003**, *206*, 2273–2280.

(33) Morgan, T. P.; Grosell, M.; Playle, R.; Wood, C. M. The time course of silver accumulation in rainbow trout during static exposure to silver nitrate: Physiological regulation or an artifact of the exposure conditions? *Aquat. Toxicol.* **2004**, *66*, 55–72.

(34) Travis, C. C.; White, R. K.; Ward, R. C. Interspecies extrapolation of pharmacokinetics. *J. Theor. Biol.* **1990**, *142*, 285–304.

(35) Garnier-Laplace, J.; Adam, C.; Lathuillière, T.; Baudin, J.-P.; Clabaut, M. A simple fish physiological model for radioecologists exemplified for  $^{54}\text{Mn}$  direct transfer and rainbow trout (*Oncorhynchus mykiss* W.). *J. Environ. Radioact.* **2000**, *49*, 35–53.

(36) Huang, Q.; Zhang, Y.; Liu, S.; Wang, W.; Luo, Y. Intraspecific scaling of resting and maximum metabolic rates of the crucian carp (*Carassius auratus*). *PLoS One* **2013**, *8*, 1–8.

(37) Karnaky, K. J., Jr.; Kinter, L. B.; Kinter, W. B.; Stirling, C. E. Teleost chloride cell II. Autoradiographic localization of gill  $\text{Na}^+/\text{K}^+$ -ATPase in killifish *Fundulus heteroclitus* adapted to low and high salinity environments. *J. Cell Biol.* **1976**, *70*, 157–177.

(38) Hossler, F. E.; Ruby, J. R.; McIlwain, T. D. The gill arch of the mullet, *Mugil cephalus*. II. Modification in surface ultrastructure and  $\text{Na}^+/\text{K}^+$ -ATPase content during adaptation to various salinities. *J. Exp. Zool.* **1979**, *208*, 399–405.

(39) Stagg, R. M.; Shuttleworth, T. J.  $\text{Na}^+/\text{K}^+$ -ATPase, ouabain binding and ouabain-sensitive oxygen consumption in gills from *Platichthys flesus* adapted to seawater and freshwater. *J. Comp. Physiol.* **1982**, *147*, 93–99.

(40) Else, P. L.; Windmill, D. J.; Markus, V. Molecular activity of sodium pumps in endotherms and ectotherms. *Am. J. Physiol.* **1996**, *271*, R1287–R1294.

(41) Laurén, D. J.; McDonald, D. G. Acclimation to copper by rainbow trout, *Salmo gairdneri*: Biochemistry. *Can. J. Fish. Aquat. Sci.* **1987**, *44*, 105–111.

(42) Dang, Z.; Lock, R. A. C.; Flik, G.; Wendelaar Bonga, S. E. Metallothionein response in gills of *Oreochromis mossambicus* exposed to copper in freshwater. *Am. J. Physiol. Regul. Integr. Comp. Physiol.* **1999**, *277*, R320–R331.

(43) McGeer, J. C.; Szebedinszky, C.; McDonald, D. G.; Wood, C. M. Effects of chronic sublethal exposure to waterborne Cu, Cd and Zn in rainbow trout 2: Tissue specific metal accumulation. *Aquat. Toxicol.* **2000**, *50*, 245–256.

(44) Monteiro, S. M.; Mancera, J. M.; Fontainhas-Fernandes, A.; Sousa, M. Copper induced alterations of biochemical parameters in the gill and plasma of *Oreochromis niloticus*. *Comp. Biochem. Physiol. Part C* **2005**, *141*, 375–383.

(45) Rombough, P. The functional ontogeny of the teleost gill: Which comes first gas or ion exchange? *Comp. Biochem. Physiol. Part A* **2007**, *148*, 732–742.

(46) Komnick, H. Chloride cells and chloride epithelia of aquatic insects. *Int. Rev. Cytol.* **1977**, *49*, 285–329.

(47) Schultz, A. G.; Ong, K. J.; MacCormack, T.; Ma, G.; Veinot, J. G. C.; Goss, G. G. Silver nanoparticles inhibit sodium uptake in juvenile rainbow trout (*Oncorhynchus mykiss*). *Environ. Sci. Technol.* **2013**, *46*, 10295–1031.